Title

Controller Synthesis for Periodic, Linear-Distributed Parameter Systems: Channel Flow Application

Journal

Journal of Guidance Control and Dynamics, 38(6)

ISSN

0731-5090

Authors

Kang, Sung M
Speyer, Jason L
Kim, John

Publication Date

2015-06-01

DOI

10.2514/1.g000418

Peer reviewed

JOURNAL OF GUIDANCE, CONTROL, AND DYNAMICS
Vol. 38, No. 6, June 2015

Controller Synthesis for Periodic, Linear-Distributed Parameter Systems: Channel Flow Application

Sung M. Kang,* Jason L. Speyer,† and John Kim†
University of California, Los Angeles, Los Angeles, California 90095-1597

DOI: 10.2514/1.G000418

A framework is presented in which temporally periodic, linear, distributed parameter systems can be converted to a time-invariant system. This conversion is key for the control of the secondary instabilities in three-dimensional channel flow induced by an upstream traveling wave of zero-net mass flux of wall transpiration. Linearized dynamical equations derived from Floquet analysis have shown that the instabilities are a direct result of the primary disturbance of the traveling wave but do not provide an analytical framework upon which to design a feedback controller. The necessary observation, although simple but subtle, is that the dynamics of the steady-state flow induced by a traveling wave must be linearized and decomposed in a frame of reference moving with the traveling wave. The resulting linear time-invariant equations are appropriate for system theoretic feedback control synthesis, i.e., H_2 and H_∞ methods. Although the linearization method produces a time-invariant linear system in the moving frame, the controller is periodic from a fixed reference frame. This approach for constructing a time-invariant system with periodic inputs is applicable to any system in which the dynamics are described as a combination of a static base and a periodic primary disturbance.

I. Introduction

IN THIS introduction, a summary of feedback control of channel flow and the origins of the periodic feedback control problem is presented. The ability to control flows has great consequences in many scientific and engineering applications and, in particular, can lead to reduced drag and increased lift. An approach to flow control, based on systems theoretic concepts, uses the governing dynamical equations to formulate feedback controllers. Studies, such as [1–9], have successfully applied systems theoretic approaches to design feedback controllers that substantially reduced drag with wall blowing/suction along the channel wall.

Although the application of systems theoretic methods affords one the ability to approach the problem of flow control in a systematic fashion, the performance of feedback control thus designed appears to be limited. Research, which focused on viscous drag reduction in a periodic channel flow, showed drag reduction in the 15 to 18% [5]. These controllers were all derived by applying modern control synthesis techniques to the spectral decomposition of the Navier–Stokes equations, linearized for small perturbations around the Poiseuille mean profile in a channel flow with a variety of feedback control cost criteria [6]. The apparent performance limit was not breached until it was discovered that a simple, sinusoidal wave of wall-normal blowing and suction at the top and bottom walls could not only drive down but sustain drag reduction in the channel [10]. Under "laminar" conditions,‡ the traveling wave functions as a pressure pump to reduce viscous drag in a channel. However, under "turbulent" conditions, the traveling wave also interacts with near-wall structures; thus, the reduction is more than purely the pumping effect [10,11]. Direct numerical simulations (DNSs) [12] initialized with a laminar flowfield show the upstream traveling wave sustained a flowfield with sublaminar drag characteristics. There are certainly positive effects of downstream traveling waves, such as increased dynamic stability of the flow [13,14], but drag is increased. Upstream traveling waves decrease dynamic stability of the flow but decrease drag. For example, DNSs initialized with a turbulent flow or with finite disturbances settled to different equilibria, which were lower than without the traveling wave but still higher than the "laminar" equilibria [see Fig. 1 for a sample of this behavior in a three-dimensional (3-D) DNS [12] of channel flows at $Re = 2000$ with traveling wave of amplitude 0.1, upstream speed of 2, and at wave number (0.5,0); note that amplitude and speed are normalized to the centerline velocity of the mean flow]. This difference in steady-state equilibria is suggestive of transition to turbulence, similar to the original problem [1] in which secondary instabilities were suppressed by systems theoretic feedback controllers.

Floquet analysis offers an explanation for the two types of equilibria by deriving the dynamics of the perturbation velocities about the periodic base flow [15]. Specifically, the perturbation velocities are characterized as having the spatial and temporal periodicity of the traveling wave. Then, the invariant portion of the periodic dynamics characterizes the stability of the traveling wave induced flow. Using a two-dimensional (2-D) Fourier decomposition in the streamwise and spanwise directions, the base flow is thus represented as a linear superposition of the Poiseuille mean profile as well as velocities (along the entire channel height not just at the wall) at the wave number of the traveling wave. This analysis clearly shows that the traveling wave induces secondary instabilities in the channel flow. Given finite amplitudes, these instabilities would transition a traveling wave induced flowfield from "laminar" to "turbulent".

Although the Floquet analysis provides a linear method by which to characterize the stability of the traveling induced flowfield, it does not directly provide system equations appropriate for control synthesis. The solution turns out to be a rather simple observation: decompose the traveling wave induced channel flow in a frame of reference moving with the traveling wave. This approach results in linear time-invariant (LTI) system equations appropriate for modern systems theoretic synthesis, discussed in Sec. II. The moving frame isolates only the temporal periodicity of the flow. The stability of these linear models matches those of the Floquet analysis and similarly couple the perturbations at different wave numbers. In Sec. III, a design and application of linear quadratic regulators (LQRs) to suppress the induced instabilities are shown to demonstrate the efficacy of using this moving-frame decomposition as a basis for feedback control synthesis. In Sec. II, the specific differences between the Floquet analysis linearized equations and the moving-frame equations are discussed. The two approaches are

Received 30 November 2013; revision received 18 August 2014; accepted for publication 20 August 2014; published online 20 January 2015.

*Visiting Scholar, Department of Mechanical and Aerospace Engineering, Box 951597 EngIV 48121.

†Professor, Department of Mechanical and Aerospace Engineering, Box 951597 EngIV 48121. Fellow AIAA.

‡The term "laminar" is used in quotations since, strictly speaking, a channel flow with an upstream traveling wave is not laminar. The terms "laminar" and "turbulent" are used in quotations in this paper to indicate flowfields without and with, respectively, finite disturbances.

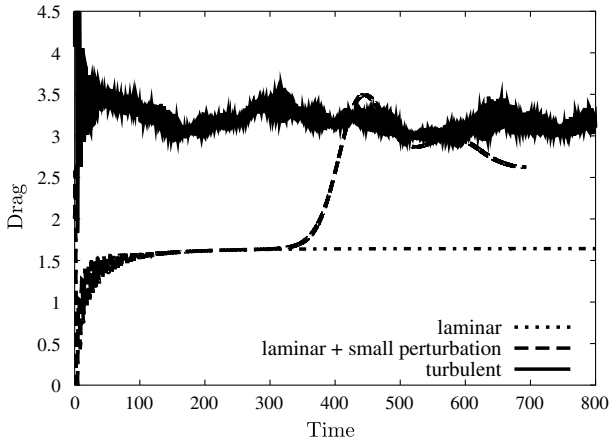

Fig. 1 History of initially purely laminar, laminar transition to turbulent flows, and fully turbulent flows induced by an upstream traveling wave.

nearly identical, but the resulting dynamical equations are different in terms of where the temporal characteristics are captured. The minor difference has an enormous affect on how easily, or even if, modern systems theoretic synthesis methods can be applied.

Although the derivation is presented in terms of the periodic channel flow, it must be stressed that this decomposition may be applied to other dynamical systems that can be described as a linear superposition of a primary disturbance and a base set of dynamics. The parallel channel flow offers such an environment. The drag reduction objective that originally motivated the discovery is, in some fashion, an afterthought for the decomposition presented. The LQR synthesis is offered to demonstrate that the linear model derived from the moving-frame decomposition is effective in DNSs. This LQR's performance in suppressing the growth of perturbation energies is shown in Sec. IV. A conclusion is presented in Sec. V.

II. Linear Modeling of Periodic Flow

The Navier–Stokes equations are linearized by considering the dynamics of only infinitesimally small perturbations around a statistically steady flow in the streamwise direction, resulting in the Orr–Sommerfeld (OS) and Squire equations. Figure 2 shows the 3-D periodic channel dimensions used in the spectral decomposition of the OS and Squire equations. In previous studies, the mean flow was assumed to be temporally and spatially static, such as Poiseuille flow. To consider the traveling wave induced flow, this work modifies this assumption by the superposition of the traveling wave induced flow as an additional component of the base flow:

$$\begin{aligned} u &= U + u_c + u' \qquad \text{(streamwise velocity)},\\ v &= v_c + v' \qquad \text{(wall-normal velocity), and}\\ w &= w_c + w' \qquad \text{(spanwise velocity)} \end{aligned} \tag{1}$$

The c subscript is introduced to indicate the velocities induced by the traveling wave. It should be assumed that in this paper all velocities are normalized to the centerline velocity of the statistically steady mean flow U. The Reynolds number for the flowfield is normalized to the centerline velocity and the channel half-height. The mean flow can be set to one of several known solutions or be obtained from DNS without any changes to the derivation steps. Furthermore, the induced velocities (u_c, v_c, and w_c) can also be obtained from DNS, or they can be approximated by the solution (with a finite amplitude) to the linearized OS and Squire equations.

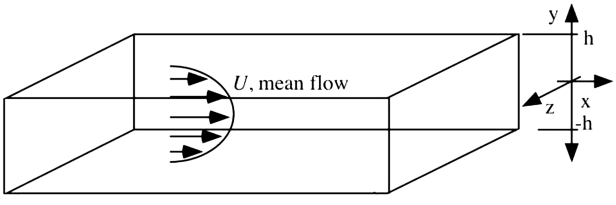

Fig. 2 Periodic channel dimensions.

A. Linear Approximation of Traveling Wave Induced Velocities

To approximate the traveling wave induced velocities using linear equations, the control input is formulated as wall-normal blowing and suction along the upper and lower walls with no net mass flux:

$$\begin{aligned} v_{\text{upper}}(x,t) &= -a\,\cos(k_x(x-ct)) \quad \text{and}\\ v_{\text{lower}}(x,t) &= a\,\cos(k_x(x-ct)) \end{aligned} \tag{2}$$

where a is a scalar representing the amplitude of suction and blowing, c is the normalized speed at which the wave travels downstream, and k_x is the streamwise wave number representing the wavelength of the traveling wave. The blowing and suction are applied on the upper and lower walls in varicose mode, in which suction (flow out of the channel) on the lower wall coincides with suction on the upper wall, the same being true for blowing (flow into the channel). Wall-normal velocity is defined as being positive in the up direction, thus the minus sign on the amplitude of the wall-normal velocity on the upper wall.

The traveling wave induced velocities u_c, v_c, and w_c are found by solving the linearized OS and Squire equations around the same mean flow as in Eq. (1). The linearized equation can be represented in state-space form as

$$\dot{\boldsymbol{x}} = \boldsymbol{A}\boldsymbol{x} + \boldsymbol{B}\boldsymbol{u} \tag{3}$$

where $\boldsymbol{x}$ represents the wall-normal perturbation velocity and vorticity, $\boldsymbol{A}$ the dynamics, $\boldsymbol{B}$ the input matrix, and $\boldsymbol{u}$ the control input. Details of this derivation can be found in previous studies, such as [1] and [2]. These system equations decouple by Fourier decomposition wave numbers, so only the subsystem corresponding to the wave number of the control input, in this case the traveling wave or $(k_x, 0)$, needs to be considered. $\boldsymbol{B}$ and $\boldsymbol{u}$ are defined to represent the effect of wall-bounded, wall-normal suction and blowing in the form of Eq. (2). One can find the value of $\boldsymbol{x}$ at any time for any known function $\boldsymbol{u}$ by the solution to Eq. (3):

$$\boldsymbol{x}(t) = e^{At}\boldsymbol{x}(0) + \int_0^t e^{A\tau}\boldsymbol{B}\boldsymbol{u}(\tau)\,\mathrm{d}\tau \tag{4}$$

Since the control input is defined as a cosine function, there is an analytical solution to Eq. (4), which is a sinusoidal function in time. The details of the derivation are presented in [16]. For the following sections, it is sufficient to describe the traveling wave induced velocity in the form (using the wall-normal velocity as the representative example)

$$v_c(t,x,y,z) = \hat{v}_c(y)e^{\hat{i}k_x(x-ct)} + \hat{v}_c^*(y)e^{-\hat{i}k_x(x-ct)} \tag{5}$$

where $\hat{v}_c$ is an appropriate amplitude function and $\hat{v}_c^*$ is its complex conjugate. It is assumed that velocities are only induced at the spatial wave number $(k_x, 0)$ of the control input wave.

B. Moving-Frame Decomposition

Floquet analysis treats the traveling wave induced velocities as a primary disturbance [17]. Linearized dynamical equations are derived by defining the perturbation velocities u', v', and w' in

the following form (again using the wall-normal velocity as the representative example):

$$v' = e^{(\hat{\imath}\alpha x + \hat{\imath}\beta z - \hat{\imath}\omega t)} \sum_{n=-\infty}^{\infty} e^{\hat{\imath} n k_x (x - ct)} \hat{v}_n(y) \tag{6}$$

Here, α and β represent perturbation wave numbers, ω is the temporal growth (or decay) rate, $\hat{v}_n(y)$ is an appropriate amplitude function, and k_x and c are the same as in Eq. (2). This is the same decomposition approach as described by [18] and [19]. The linear analysis by [15] also shows that these linearized equations do demonstrate secondary instabilities induced by the traveling wave. However, the decomposition does not provide a set of ordinary differential equations (ODEs) suitable for feedback control design.

Primarily, both the temporal and spatial periodicity of the traveling wave is represented in the perturbation dynamics. Systems theoretic synthesis approaches require that the perturbation dynamics be only of time. Floquet theory does offer a method by which the temporally periodic dynamics can be extracted [20]. However, this approach is numerically intractable due to the large number of system equations that is typical with the decomposition of flowfield dynamics.

Here is presented an alternative decomposition to directly and simply capture the temporal periodicity induced by the traveling wave. Instead of directly determining the periodic dynamics by calculating the transition function over a period, the decomposition is performed in a frame of reference that moves with the traveling wave. This approach results directly in time-invariant system equations.

The coordinate frame is made to move with the traveling wave:

$$t' = t, \qquad x' = x - ct, \quad y' = y, \quad \text{and} \qquad z' = z \tag{7}$$

Note that the $'$ is used here to represent the moving frame in relation to the fixed or laboratory frame. The traveling wave control input is defined in the new frame as

$$v_{\text{upper}}(x', t) = -a\,\cos(k_x x') \quad \text{and}$$
$$v_{\text{lower}}(x', t) = a\,\cos(k_x x')$$
$$\text{or}$$
$$v_c(t, x, y, z) = \hat{v}_c(y) e^{\hat{\imath} k_x x'} + \hat{v}_c^*(y) e^{-\hat{\imath} k_x x'} \tag{8}$$

The perturbation velocities are now defined as (again using the wall-normal velocity as an example):

$$v' = \sum_{\substack{n=-N,\\ m=-M}}^{N,M} \hat{v}(t', y') e^{\hat{\imath} n \alpha_0 x' + \hat{\imath} m \beta_0 z'} \tag{9}$$

where α_0 and β_0 represent the fundamental wave numbers of the decomposition and $\hat{v}(t', y')$ is, again, an appropriate amplitude function but now also a function of time (6). The temporal dynamical behaviors are strictly those that are independent of the periodicity of the traveling wave. Furthermore, α_0 will need to be small enough so that k_x can be described as a whole number multiple of it, i.e., $k_x = n_c \alpha_0$. If $n_c > 1$ or $\alpha_0 < k_x$, subharmonic frequencies can be studied. For the reader's convenience, the linearized velocity equations induced by the traveling wave are given in Appendix A, and the decomposition into ordinary differential equations appropriate for state-space equations is described in Appendix B.

The coupling between the wave numbers is not as obvious as the decomposition of the Floquet analysis described previously, in which the coupling is explicit in the definition of the perturbation velocity (6). The coupling now arises with the projection made to decompose the governing equations (see Appendix B), which is a projection made with known basis functions,

$$\langle \cdot, \Gamma_\ell(y) e^{\hat{\imath} h \alpha_0 x' + \hat{\imath} j \beta_0 z'} \rangle \tag{10}$$

where $\Gamma_\ell(y)$ is an appropriate basis function for the decomposition in the wall-normal direction, the brackets denote the inner product with these basis functions, and h and j are whole number indices. Since k_x will be coincident to some values of n in Eq. (9), the previous inner product will allow, for example, three terms to survive: perturbation velocities at wave numbers (n, m), $(n - n_c, m)$, and $(n + n_c, m)$. In state-space form, this means the linear equations will have, or can be easily made to have, the following block form:

$$\frac{\mathrm{d}}{\mathrm{d}t}\begin{bmatrix} \vdots \\ \boldsymbol{x}_{-1} \\ \boldsymbol{x}_0 \\ \boldsymbol{x}_1 \\ \vdots \end{bmatrix} = \begin{bmatrix} \ddots & & & & & & \\ \boldsymbol{M}_{-1} & \boldsymbol{A}_{-1} & \boldsymbol{P}_{-1} & & & & \\ & \boldsymbol{M}_0 & \boldsymbol{A}_0 & \boldsymbol{P}_0 & & & \\ & & \boldsymbol{M}_1 & \boldsymbol{A}_1 & \boldsymbol{P}_1 & & \\ & & & & & \ddots & \end{bmatrix}\begin{bmatrix} \vdots \\ \boldsymbol{x}_{-1} \\ \boldsymbol{x}_0 \\ \boldsymbol{x}_1 \\ \vdots \end{bmatrix} \tag{11}$$

Simplified notations for brevity and clarity of presentation are used, in which the -1 subscript represents perturbation at the wave number $(n - n_c, m)$, the 0 subscript the wave number (n, m), and the 1 subscript the wave number $(n + n_c, m)$. With the exception of this coupling between wave numbers, the same linear state-space equations as Eq. (3) can be constructed,

$$\dot{\bar{\boldsymbol{x}}} = \bar{\boldsymbol{A}}\,\bar{\boldsymbol{x}} + \bar{\boldsymbol{B}}\,\bar{\boldsymbol{u}} \tag{12}$$

where $\bar{\boldsymbol{x}}$ is the collection of $\boldsymbol{x}$ at different wave numbers as in Eq. (11), $\bar{\boldsymbol{A}}$ is the time-invariant dynamical matrix, $\bar{\boldsymbol{u}}$ is a similar collection of the $\boldsymbol{u}$ in Eq. (3), and $\bar{\boldsymbol{B}}$ is the time-invariant input matrix that couples the inputs at different wave numbers. Appendix B presents more details on how the state-space equations are derived from the partial differential equations. The coupling shown in $\bar{\boldsymbol{A}}$ is similar to coupling by Floquet analysis of the traveling wave induced flow dynamics. In fact, picking α_0 to equal k_x or $n_c = 1$, the same stability characteristics are found from $\bar{\boldsymbol{A}}$ as are found by the secondary stability analysis. However, the LTI state-space equations (or system matrices) derived by this approach are appropriate for any systems theoretic approach because they are linear time-invariant state-space equations.

III. Feedback Transition Control of Periodic Flow

This work designs a LQR to suppress the induced secondary instabilities using the state-space equations (12) found using the projection (10) on the decomposition described in Sec. II.B. To derive the system matrices, one takes a spectral decomposition of the dynamics in a $4\pi h \times 2h \times 4\pi h/3$ channel (streamwise, wall-normal, and spanwise directions in a channel as shown in Fig. 2), where h has been normalized to 1. A 2-D Fourier decomposition is taken in the streamwise and spanwise directions, for which 64 wave numbers are assigned in each direction. The decomposition in the wall-normal direction is taken by a 97-function Galerkin projection. As in many previous studies [1,21], the control is defined as zero-net mass-flux, wall-bounded, wall-normal blowing and suction. In the presence of the traveling wave, the feedback control would be linearly superpositioned with the traveling wave. The coupled system is truncated to include five perturbation wave number states, i.e., wave numbers $(n - 2 * n_c)$, $(n - n_c)$, n, $(n + n_c)$, and $(n + 2 * n_c)$.

Based on the coupled dynamics of Eq. (12) in a moving coordinate frame, the linear-quadratic problem is to find a feedback control $\bar{u}$ that minimizes the quadratic cost

$$J^o = \min_{\bar{\boldsymbol{u}}} \int_t^\infty (\bar{\boldsymbol{x}}^\top \bar{\boldsymbol{Q}}\,\bar{\boldsymbol{x}} + \gamma \bar{\boldsymbol{u}}^\top \bar{\boldsymbol{R}}\,\bar{\boldsymbol{u}})\,\mathrm{d}\tau \tag{13}$$

subject to Eq. (12). One can use γ as a tuning parameter, and $\bar{\boldsymbol{Q}}$ and $\bar{\boldsymbol{R}}$ are taken as the identity. This is an arbitrary selection and does not represent a quantity such as perturbation energy or Reynolds shear stress. The proper selection of cost functions would be appropriate for

a larger study into a drag reduction in a parallel channel flow. This arbitrary selection is made here since the primary objective of this study is to present the usefulness of the moving-frame decomposition in providing a framework to apply systems theoretic synthesis methods to spatially and temporally periodic dynamical systems. Truncating the state model at five coupled wave numbers is also an arbitrary decision.

Using these system matrices in Eq. (12), one can obtain an LQR controller,

$$\bar{\boldsymbol{u}} = -\bar{\boldsymbol{K}}\,\bar{\boldsymbol{x}} \tag{14}$$

which is determined from the usual linear quadratic control synthesis methods. Since this study assumes that the state is known and there is no process noise, then the LQR is an appropriate controller given its inherent gain and phase margins due to the circle criterion [22]. These feedback control gains found here are temporally constant in a moving frame of reference but periodic in a fixed frame of reference. Perturbations and control inputs that are not periodic in the moving frame of reference become periodic in the fixed frame. This requires a transformation, block diagonal in the periodic frequencies of the five coupled wave number states, on both the control and state from the moving frame to the fixed frame. So although LTI control synthesis techniques are being used, it is important to keep in mind that the dynamical system, coefficients, and control gains are, in fact, periodic in the fixed frame of reference.

Figure 3 shows the performance without and with a LQR designed for and applied to a flow at $Re = 5000$ with a traveling wave of amplitude 0.008 and upstream speed 2 at the first streamwise wave number. The DNS is performed by a pseudospectral code similar to the one used by [12]. For the DNS, a $64 \times 97 \times 64$ grid point is taken, but one should note that the wall-normal decomposition is a collocation method in the DNS. To apply the feedback control gains calculated using the Galerkin projection decomposed system matrices, the DNS perturbation state is converted from the Galerkin projection state to the collocation state. This is accomplished by a straightforward linear transformation that is not detailed here. Since full state feedback, assumed for LQR, is not practically possible for flow control, these LQR results should be seen as demonstration, since, in a complete study of a drag reduction, a whole host of other factors, including cost functional, system size, and estimators, would need to be considered. These results are, however, quite effective in demonstrating that linear system models derived using the presented moving-frame decomposition provide a good basis for synthesizing feedback control for a highly nonlinear system. Furthermore, it is possible to use the same mathematical framework to design systems theoretic estimators, such as Kalman filters [9].

IV. Suppression of Growing Perturbations

Given the success of the simple application described in Sec. III (see Fig. 3), DNS experiments were conducted to test the ability of the moving-frame LQR to suppress the secondary instabilities for a larger amplitude traveling wave induced flow. As described in the previous section, the feedback control is designed on a $64 \times 97 \times 64$ spectral decomposition system matrix in which the wall-normal direction is decomposed by a Galerkin projection, while the DNS is based on collocation points. The computational domain remains $4\pi h \times 2h \times 4\pi h/3$ with the same grid point of $64 \times 97 \times 64$, with a collocation method used to decompose the velocities in the wall-normal direction. The conversion from Galerkin projection to collocation state is made inline during the simulation.

For the results presented in this section, a higher amplitude traveling wave were picked because the expectation is that the higher amplitude would pose a greater challenge for the moving-frame LQR. The derivation is dependent on an assumption of small amplitude perturbations, for both the traveling wave induced velocities and the perturbation velocities. There is a real concern for the efficacy of any controller designed on systems derived from such

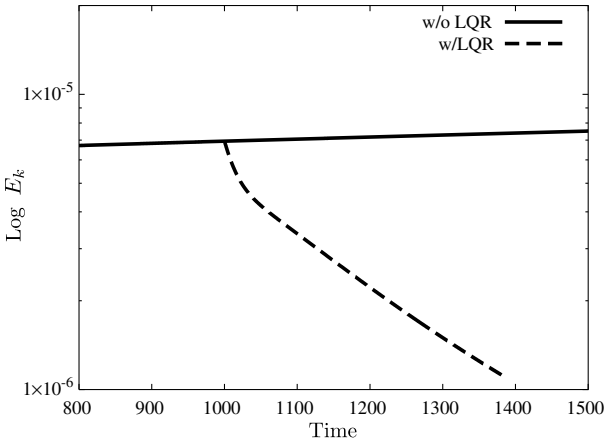

Fig. 3 The perturbation energy at the first spanwise wave number.

assumptions. For the flow at $Re = 5000$ with a traveling wave with amplitude 0.03 and speed $c = -2$ at the perturbation wave number (0.5, 0), one can observe instabilities induced in the linear, coupled-state system for the first six spanwise wave numbers. Initializing the DNS with a Poiseuille flow with randomized perturbations of amplitude 10^{-4} demonstrates these instabilities quite nicely (see Fig. 4 for a traveling wave of amplitude 0.03 and with and without LQR). One can also observe that without a finite disturbance the uncontrolled flowfield remains "laminar". At the log scale of Fig. 4, the undisturbed flow's total perturbation energy overlaps with those of the flowfields to which a LQR controller has been applied. The LQR controllers are synthesized on linear models derived using the moving-frame decomposition described in Sec. II.B for each of the spanwise wave number states with instabilities. These systems are truncated to the five wave number models. Two LQRs are synthesized using different weighting in the cost function (13). The cost function used in designing the LQRs is still the arbitrary selection of identity matrices for $\bar{\boldsymbol{Q}}$ and $\bar{\boldsymbol{R}}$, roughly representing the square of the perturbation velocities. The controller is turned on at $t = 500$. The results are shown in Figs. 4 and 5.

Even with the simple cost function, the LQR control is quite effective in suppressing the growth of perturbation velocities. Figure 4 shows the time history of the total perturbation energy of the flow. The LQRs applied at the first six spanwise wave numbers suppresses the induced instabilities so that their perturbation energy time histories collapse to the energy of the traveling wave control itself. Figures 5a–5f for channel flow with a traveling wave of amplitude 0.03 more clearly show the LQR wall-bounded controller's ability to damp out the secondary instabilities; these are perturbation energies at only the first six spanwise wave numbers. All of these plots are of the log of the perturbation energy vs time.

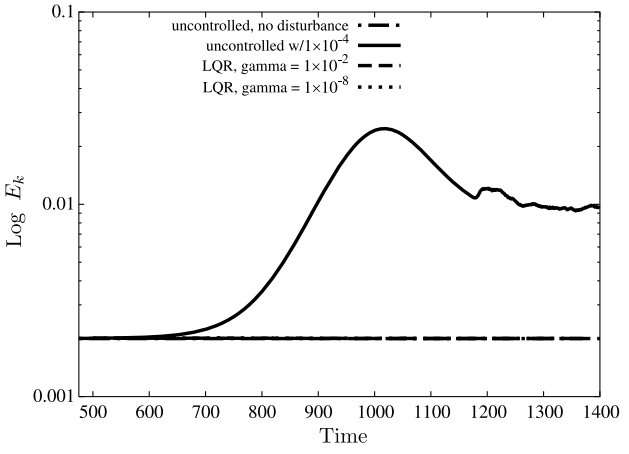

Fig. 4 The total perturbation energy for channel flow.

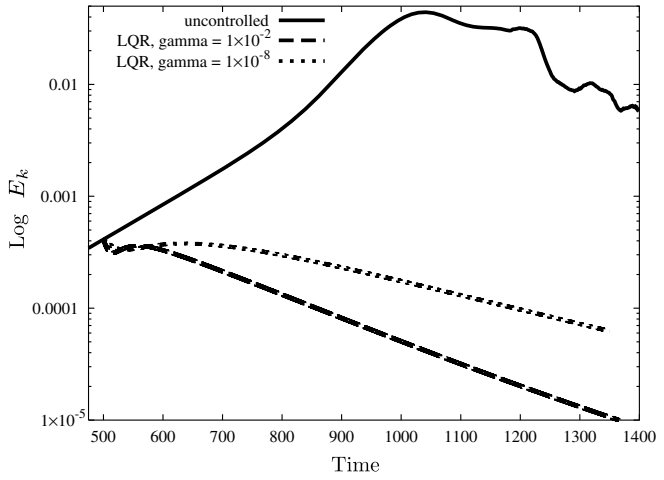

a) Spanwise waven umber m = 1

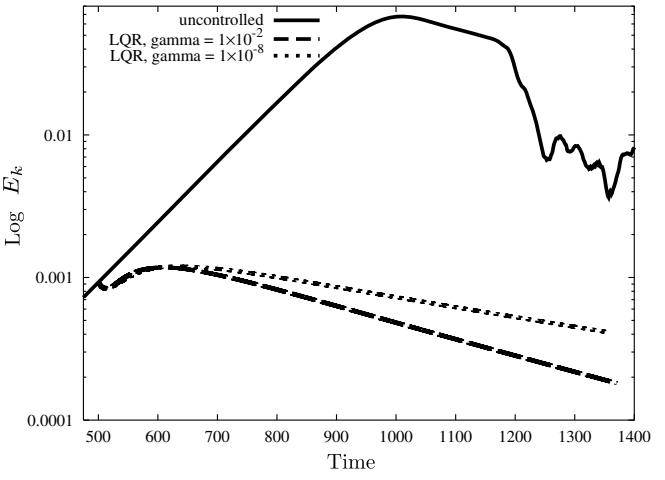

b) Spanwise wave number m = 2

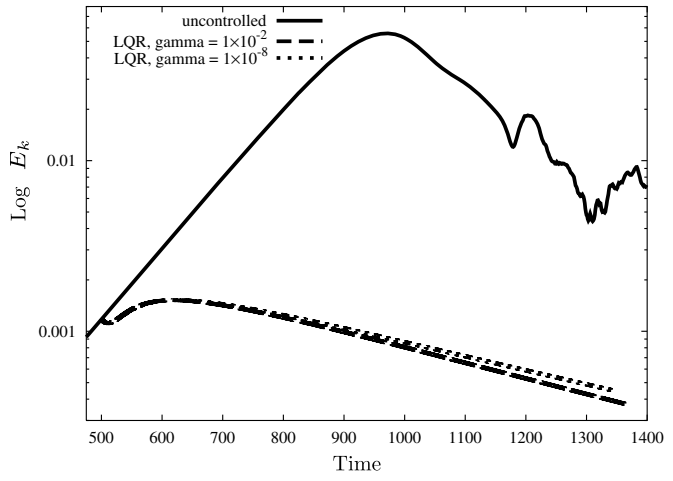

c) Spanwise wave number m = 3

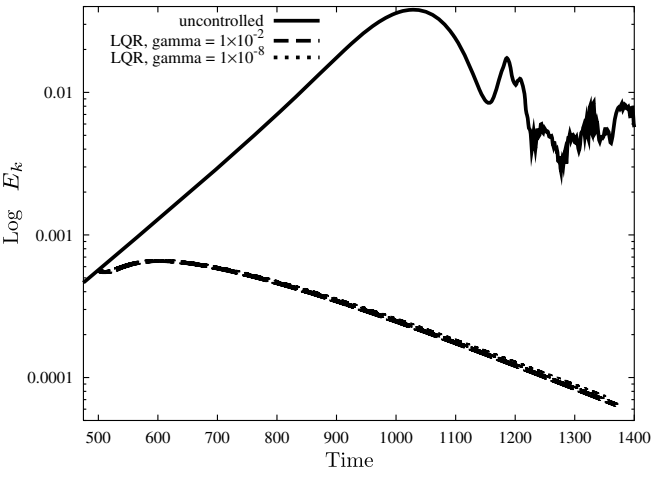

d) Spanwise wave number m = 4

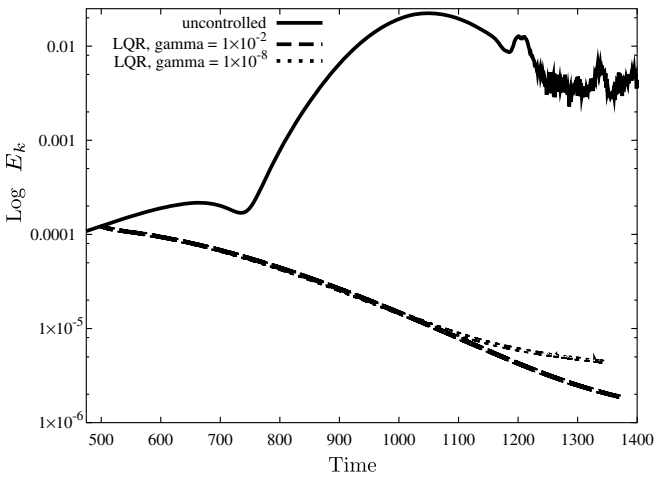

e) Spanwise wave number m = 5

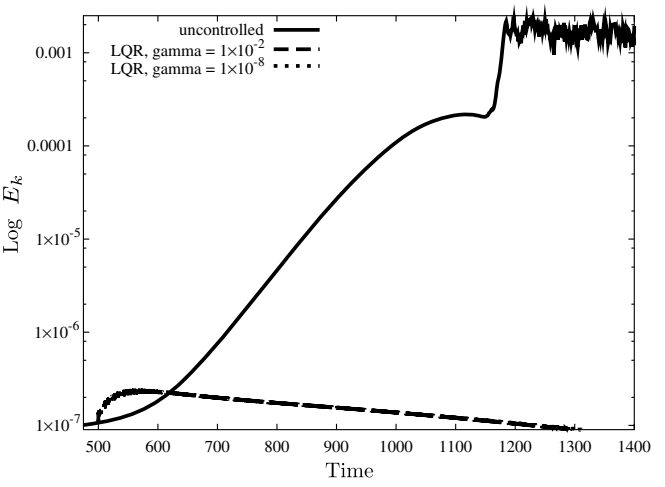

f) Spanwise wave number m = 6

Fig. 5 The perturbation energy at the first six spanwise wave numbers.

V. Conclusions

The moving-frame decomposition, in the context of perturbation growth in parallel channel flows, provides a framework in which systems theoretic feedback control synthesis can be applied to periodic dynamical systems. Decomposing the governing equations in a moving frame of reference results in linear time-invariant (LTI) system equations that are appropriate for systems theoretic control synthesis. These system matrix equations predict the same stability characteristics as Floquet analysis, but the temporal periodicity induced by the traveling wave is handled by the moving-frame decomposition. This paper has shown that linear quadratic regulator (LQR) control, synthesized using the moving-frame decomposition linear model, can suppress the growing perturbation energy of unstable modes induced by small (and larger) amplitude traveling waves.

The moving-frame decomposition presented in this study does not address the totality of feedback control needed to suppress transition

or viscous drag in a channel flow. Rather, this study presents an avenue to handle large, complex dynamical systems that can be described as a linear combination of base and primary disturbance dynamics. The terminologies become much clearer when described in the context of parallel flowfields. In this context, the terms "base flow" and "primary disturbance" have specific meanings that help clarify the discussion of the moving-frame decomposition. Of course, the discovery has also been made while researching the application of systems theoretic control methods for channel flow control. The apposite result presented is that, although Floquet analysis provides an explanation of growth or decay rates, it does not provide the temporal dynamics needed by systems theoretic synthesis methods to design feedback controllers.

The decomposition of the dynamics in a moving frame does not preclude the application of methodologies already developed for LTI systems, such as Kalman filters to estimate the flow state. The derivation of such a linear estimator is not presented here specifically but rather implicitly through the duality with LQR controller design methodology. However, demonstration of an estimator for channel flow is quite challenging and will be addressed in future work. The purpose of this study is to present a mathematical framework to allow the use of linear systems theoretic approaches to temporally and spatially periodic systems.

Appendix A: Traveling Wave Induced Flow Equations

Applying the flow velocity definitions (1) (as well as the flow pressure, which is not explicitly shown) directly in the Navier–Stokes momentum equations, the parts associated strictly with the base component (in this case U as well as u_c, v_c, and w_c) are subtracted out so that one is left with only the dynamics of the perturbations. In a sense, the base flow is being treated as a known quantity that is not affected by the perturbation values.

Given the Navier–Stokes momentum equations for an incompressible flow, the momentum equations in the streamwise, wall-normal, and spanwise directions are

$$\frac{\partial}{\partial t}(U+u_c+u')+(U+u_c+u')\frac{\partial}{\partial x}(U+u_c+u') + (v_c+v')\frac{\partial}{\partial y}(U+u_c+u')+(w_c+w')\frac{\partial}{\partial z}(U+u_c+u') = -\frac{\partial p}{\partial x}+\frac{1}{Re}\nabla^2(U+u_c+u') \tag{A1}$$

$$\frac{\partial}{\partial t}(v_c+v')+(U+u_c+u')\frac{\partial}{\partial x}(v_c+v') + (v_c+v')\frac{\partial}{\partial y}(v_c+v')+(w_c+w')\frac{\partial}{\partial z}(v_c+v') = -\frac{\partial p}{\partial y}+\frac{1}{Re}\nabla^2(v_c+v') \tag{A2}$$

$$\frac{\partial}{\partial t}(w_c+w')+(U+u_c+u')\frac{\partial}{\partial x}(w_c+w') + (v_c+v')\frac{\partial}{\partial y}(w_c+w')+(w_c+w')\frac{\partial}{\partial z}(w_c+w') = -\frac{\partial p}{\partial z}+\frac{1}{Re}\nabla^2(w_c+w') \tag{A3}$$

where p is the pressure field in the channel. Now, noting that u_c, v_c, and w_c are also considered to be part of the base flow, the base flow momentum equations are as follows (again by streamwise, wall-normal, and spanwise directions):

$$\frac{\partial U}{\partial t}+\frac{\partial u_c}{\partial t}+U\frac{\partial U}{\partial x}+U\frac{\partial u_c}{\partial x}+u_c\frac{\partial U}{\partial x}+u_c\frac{\partial u_c}{\partial x} + v_c\frac{\partial U}{\partial y}+v_c\frac{\partial u_c}{\partial y}+w_c\frac{\partial U}{\partial z}+w_c\frac{\partial u_c}{\partial z} = -\frac{\partial(P+p_c)}{\partial x}+\frac{1}{Re}\nabla^2(U+u_c) \tag{A4}$$

$$\frac{\partial v_c}{\partial t}+U\frac{\partial v_c}{\partial x}+u_c\frac{\partial v_c}{\partial x}+v_c\frac{\partial v_c}{\partial y}+w_c\frac{\partial v_c}{\partial z} = -\frac{\partial(P+p_c)}{\partial y}+\frac{1}{Re}\nabla^2(v_c) \tag{A5}$$

$$\frac{\partial w_c}{\partial t}+U\frac{\partial w_c}{\partial x}+u_c\frac{\partial w_c}{\partial x}+v_c\frac{\partial w_c}{\partial y}+w_c\frac{\partial w_c}{\partial z} = -\frac{\partial(P+p_c)}{\partial z}+\frac{1}{Re}\nabla^2(w_c) \tag{A6}$$

It should be noted that u_c, v_c, and w_c do not necessarily satisfy the previous equations since they were all derived (or gathered from DNS) with the assumption that u_c, v_c, and $w_c \ll U$. These particular dynamical equations are for any flow for which the velocities can be expressed as in Eq. (1). Subtracting Eqs. (A4–A6) from Eqs. (A1–A3) and eliminating negligible terms, i.e., the perturbation quadratic terms, results in the following linear perturbation equations about the traveling wave induced steady-state flow:

$$\frac{\partial u'}{\partial t}+U\frac{\partial u'}{\partial x}+u_c\frac{\partial u'}{\partial x}+u'\frac{\partial U}{\partial x}+u'\frac{\partial u_c}{\partial x}+v_c\frac{\partial u'}{\partial y} + v'\frac{\partial U}{\partial y}+v'\frac{\partial u_c}{\partial y}+w_c\frac{\partial u'}{\partial z}+w'\frac{\partial U}{\partial z}+w'\frac{\partial u_c}{\partial z} = -\frac{\partial p'}{\partial x}+\frac{1}{Re}\nabla^2(u') \tag{A7}$$

$$\frac{\partial v'}{\partial t}+U\frac{\partial v'}{\partial x}+u_c\frac{\partial v'}{\partial x}+u'\frac{\partial v_c}{\partial x}+v_c\frac{\partial v'}{\partial y}+v'\frac{\partial v_c}{\partial y}+w_c\frac{\partial v'}{\partial z}+w'\frac{\partial v_c}{\partial z} = -\frac{\partial p'}{\partial y}+\frac{1}{Re}\nabla^2(v') \tag{A8}$$

$$\frac{\partial w'}{\partial t}+U\frac{\partial w'}{\partial x}+u_c\frac{\partial w'}{\partial x}+u'\frac{\partial w_c}{\partial x}+v_c\frac{\partial w'}{\partial y}+v'\frac{\partial w_c}{\partial y}+w_c\frac{\partial w'}{\partial z}+w'\frac{\partial w_c}{\partial z} = -\frac{\partial p'}{\partial z}+\frac{1}{Re}\nabla^2(w') \tag{A9}$$

One can now explicitly assume that $u' \ll U$ and that $u' \ll u_c$. It should be noted that the derivation of the dynamical equations up to this point does not necessarily require that $u_c \ll U$, only that the velocities can be described as Eq. (1). Furthermore, U of the base flow has not been defined. Defining U to be the Poiseuille profile, $1-y^2$, streamwise momentum equation (A7) further reduces to (or any statistically steady-state mean with no change in the streamwise, spanwise, and temporal directions)

$$\frac{\partial u'}{\partial t}+U\frac{\partial u'}{\partial x}+u_c\frac{\partial u'}{\partial x}+u'\frac{\partial u_c}{\partial x}+v_c\frac{\partial u'}{\partial y}+v'\frac{\partial U}{\partial y} + v'\frac{\partial u_c}{\partial y}+w_c\frac{\partial u'}{\partial z}+w'\frac{\partial u_c}{\partial z} = -\frac{\partial p'}{\partial x}+\frac{1}{Re}\nabla^2(u') \tag{A10}$$

Equations (A10), (A8), and (A9) match exactly that of [19]. These equations can be further manipulated to approximate the Orr–Sommerfeld and Squire equations by the following:

Orr–Sommerfeld equivalent: $\frac{\partial^2(\text{A8})}{\partial x^2}+\frac{\partial^2(\text{A8})}{\partial z^2}-\frac{\partial^2(\text{A10})}{\partial x\partial y}-\frac{\partial^2(\text{A9})}{\partial y\partial z}$

and Squire equivalent: $\frac{\partial(\text{A10})}{\partial z}-\frac{\partial(\text{A9})}{\partial x}$

Further manipulation results in the equations that describe the perturbation dynamics,

$$\begin{aligned}
&\frac{\partial}{\partial t}\nabla^2 v' + U\frac{\partial}{\partial x}\nabla^2 v' - \frac{\mathrm{d}^2 U}{\mathrm{d}y^2}\frac{\partial v'}{\partial x} + u_c\frac{\partial}{\partial x}\nabla^2 v' + v_c\frac{\partial}{\partial y}\nabla^2 v' \\
&\quad + w_c\frac{\partial}{\partial z}\nabla^2 v' + \left(\frac{\partial}{\partial x}\nabla^2 v_c\right)u' + \left(\frac{\partial}{\partial y}\nabla^2 v_c\right)v' + \left(\frac{\partial}{\partial z}\nabla^2 v_c\right)w' \\
&\quad + \frac{\partial v_c}{\partial y}\nabla^2 v' + (\nabla^2 v_c)\frac{\partial v'}{\partial y} - 2\frac{\partial\omega_{xc}}{\partial x}\frac{\partial u'}{\partial z} - 2\frac{\partial u_c}{\partial z}\frac{\partial\omega_x'}{\partial x} + 2\frac{\partial\omega_{zc}}{\partial z}\frac{\partial w'}{\partial x} \\
&\quad + 2\frac{\partial w_c}{\partial x}\frac{\partial\omega_z'}{\partial z} + 2\frac{\partial\omega_{zc}}{\partial x}\frac{\partial u'}{\partial x} + 2\frac{\partial u_c}{\partial x}\frac{\partial\omega_z'}{\partial x} - 2\frac{\partial w_c}{\partial z}\frac{\partial\omega_x'}{\partial z} - 2\frac{\partial\omega_{xc}}{\partial z}\frac{\partial w'}{\partial z} \\
&\quad + \frac{\partial v_c}{\partial x}\left(\frac{\partial\omega_z'}{\partial y} + \frac{\partial\omega_y'}{\partial z}\right) + \left(\frac{\partial\omega_{zc}}{\partial y} + \frac{\partial\omega_{yc}}{\partial z}\right)\frac{\partial v'}{\partial x} \\
&\quad - \frac{\partial v_c}{\partial z}\left(\frac{\partial\omega_x'}{\partial y} + \frac{\partial\omega_y'}{\partial x}\right) - \left(\frac{\partial\omega_{xc}}{\partial y} + \frac{\partial\omega_{yc}}{\partial x}\right)\frac{\partial v'}{\partial z} \\
&\quad = \frac{1}{Re}\nabla^2\nabla^2 v' \qquad \text{(A11)}
\end{aligned}$$

$$\begin{aligned}
&\frac{\partial}{\partial t}\omega_y' + U\frac{\partial}{\partial x}\omega_y' + \frac{\mathrm{d}U}{\mathrm{d}y}\frac{\partial v'}{\partial z} + u_c\frac{\partial}{\partial x}\omega_y' + v_c\frac{\partial}{\partial y}\omega_y' + w_c\frac{\partial}{\partial z}\omega_y' \\
&\quad + \left(\frac{\partial}{\partial x}\omega_{yc}\right)u' + \left(\frac{\partial}{\partial y}\omega_{yc}\right)v' + \left(\frac{\partial}{\partial z}\omega_{yc}\right)w' - \frac{\partial v_c}{\partial y}\omega_y' \\
&\quad - \omega_{yc}\frac{\partial v'}{\partial y} + \frac{\partial u_c}{\partial y}\frac{\partial v'}{\partial z} + \frac{\partial v_c}{\partial z}\frac{\partial u'}{\partial y} - \frac{\partial v_c}{\partial x}\frac{\partial w'}{\partial y} - \frac{\partial w_c}{\partial y}\frac{\partial v'}{\partial x} \\
&\quad = \frac{1}{Re}\nabla^2\omega_y' \qquad \text{(A12)}
\end{aligned}$$

where ω_x, ω_y, and ω_z are the component of vorticity. Equation (A11) is the equivalent to the Orr–Sommerfeld equation although u' and w' are still involved as is the case with Eq. (A12). The fact that these equations are not solely dependent on v' and ω_y' is only of marginal concern; once the velocities are decomposed, one can make the appropriate substitutions to reformulate them to be so (see Appendix B).

Appendix B: Spectral Decomposition in Moving Frame

Equations (A11) and (A12) represent the linearized dynamics of small perturbations about a base flow that is described as a linear superposition of a primary disturbance (traveling wave in this particular case) and a mean flow in a channel. Linearity is gained by assuming that the perturbation is too small to affect both the primary disturbance and the mean flow. To design control laws, one needs to derive ODEs from these partial differential equations.

The ODEs are derived by decomposing the velocities with a Fourier expansion in the streamwise and spanwise directions and a Galerkin projection expansion in the wall-normal direction (other projections and expansion can, of course, be used) in a frame of reference moving with the wave [repeating Eq. (7) here for convenience]:

$$t' = t, \quad x' = x - ct, \quad y' = y, \quad \text{and} \quad z' = z \qquad \text{(B1)}$$

The moving-frame reference changes the partial derivatives for the partial differential equations (A11) and (A12):

$$\frac{\partial}{\partial t} = \frac{\partial}{\partial t'} - c_t\frac{\partial}{\partial x'}, \quad \frac{\partial}{\partial x} = \frac{\partial}{\partial x'}, \quad \frac{\partial}{\partial y} = \frac{\partial}{\partial y'}, \quad \text{and} \quad \frac{\partial}{\partial z} = \frac{\partial}{\partial z'} \qquad \text{(B2)}$$

To limit confusion, the apostrophe is dropped when referring to the coordinate variables in the moving frame (i.e., x is used instead of x', t is t', y is y', and z is z') in the remaining part of this discussion. The apostrophe will still be used to refer to the perturbation flow properties. This distinction will need to be kept in mind when the partial differential equations are decomposed into ODEs.

The perturbation dynamical equations (A11) and (A12) are decomposed into ODEs by using the following expansions in the moving frame:

$$u_c(t,x,y,z) = 1/2(\hat{u}_c(y,t)e^{\hat{i}k_x x} + \hat{u}_c^*(y,t)e^{-\hat{i}k_x x}) \qquad \text{(B3)}$$

$$v_c(t,x,y,z) = 1/2(\hat{v}_c(y,t)e^{\hat{i}k_x x} + \hat{v}_c^*(y,t)e^{-\hat{i}k_x x}) \qquad \text{(B4)}$$

$$w_c(t,x,y,z) = 1/2(\hat{w}_c(y,t)e^{\hat{i}k_x x} + \hat{w}_c^*(y,t)e^{-\hat{i}k_x x}) \qquad \text{(B5)}$$

$$\begin{aligned}
\omega_{xc}(t,x,y,z) &= \frac{\partial w_c(t,x,y,z)}{\partial y} - \frac{\partial v_c(t,x,y,z)}{\partial z} \\
&= \frac{1}{2}\left[\left(\hat{i}\frac{\partial\hat{w}_c(y,t)}{\partial y} - \hat{i}k_z\hat{v}_c(y,t)\right)e^{\hat{i}k_x x}\right. \\
&\quad \left. - \left(\hat{i}\frac{\partial\hat{w}_c^*(y,t)}{\partial y} - \hat{i}k_z\hat{v}_c^*(y,t)\right)e^{-\hat{i}k_x x}\right] \qquad \text{(B6)}
\end{aligned}$$

$$\begin{aligned}
\omega_{yc}(t,x,y,z) &= \frac{\partial u_c(t,x,y,z)}{\partial z} - \frac{\partial w_c(t,x,y,z)}{\partial x} \\
&= \frac{1}{2}\left[\left(\hat{i}k_z\hat{u}_c(y,t) - \hat{i}k_x\hat{w}_c(y,t)\right)e^{\hat{i}k_x x}\right. \\
&\quad \left. - \left(\hat{i}k_z\hat{u}_c^*(y,t) - \hat{i}k_x\hat{w}_c^*(y,t)\right)e^{-\hat{i}k_x x}\right] \qquad \text{(B7)}
\end{aligned}$$

$$\begin{aligned}
\omega_{zc}(t,x,y,z) &= \frac{\partial v_c(t,x,y,z)}{\partial x} - \frac{\partial u_c(t,x,y,z)}{\partial y} \\
&= \frac{1}{2}\left[\left(\hat{i}k_x\hat{v}_c(y,t) - \hat{i}\frac{\partial\hat{u}_c(y,t)}{\partial y}\right)e^{\hat{i}k_x x}\right. \\
&\quad \left. - \left(\hat{i}k_x\hat{v}_c^*(y,t) - \hat{i}\frac{\partial\hat{v}_c^*(y,t)}{\partial y}\right)e^{-\hat{i}k_x x}\right] \qquad \text{(B8)}
\end{aligned}$$

$$\begin{aligned}
&u'(t,x,y,z) \\
&= \frac{1}{2}\sum_{nm}\frac{-\hat{i}}{\gamma^2}\left(m\beta_0\hat{\omega}_{ynm}(y,t) - n\alpha_0\frac{\partial\hat{v}(y,t)}{\partial y}\right)e^{\hat{i}(n\alpha_0 x + m\beta_0 z)} \qquad \text{(B9)}
\end{aligned}$$

$$v'(t,x,y,z) = \frac{1}{2}\sum_{nm}\hat{v}(y,t)e^{\hat{i}(n\alpha_0 x + m\beta_0 z)} \qquad \text{(B10)}$$

$$\begin{aligned}
&w'(t,x,y,z) \\
&= \frac{1}{2}\sum_{nm}\frac{\hat{i}}{\gamma^2}\left(n\alpha_0\hat{\omega}_{ynm}(y,t) + m\beta_0\frac{\partial\hat{v}(y,t)}{\partial y}\right)e^{\hat{i}(n\alpha_0 x + m\beta_0 z)} \qquad \text{(B11)}
\end{aligned}$$

$$\begin{aligned}
&\omega_x'(t,x,y,z) \\
&= \frac{1}{2}\sum_{nm}\left[\frac{\hat{i}}{\gamma^2}\left(n\alpha_0\frac{\partial\hat{\omega}_{ynm}(y,t)}{\partial y} + m\beta_0\frac{\partial^2\hat{v}(y,t)}{\partial y^2}\right) - \hat{i}m\beta_0\hat{v}(y,t)\right] \\
&\times e^{\hat{i}(n\alpha_0 x + m\beta_0 z)} \qquad \text{(B12)}
\end{aligned}$$

$$\omega_y'(t,x,y,z) = \frac{1}{2}\sum_{nm}\hat{\omega}_{ynm}(y,t)e^{\hat{i}(n\alpha_0 x + m\beta_0)} \qquad \text{(B13)}$$

$$\omega'_z(t,x,y,z) = \frac{1}{2}\sum_{nm}\left[\frac{\hat{i}}{\gamma^2}\left(m\beta_0\frac{\partial\hat{\omega}_{ynm}(y,t)}{\partial y} - n\alpha_0\frac{\partial^2\hat{v}(y,t)}{\partial y^2}\right) + \hat{i}n\alpha_0\hat{v}(y,t)\right] \times e^{\hat{i}(n\alpha_0 x + m\beta_0 z)} \tag{B14}$$

Note that $\sum_{nm}$ is introduced as a shorthand notation for summation over $n = -N \to N$ and $m = -M \to M$, introduced with the definition (9). Furthermore, this work used the definition of vorticity to describe all the quantities in terms of v' and ω'_y. Substituting these definitions into Eqs. (A11) and (A12) results in ODEs for the three-dimensional channel flow that can be cast into state-space form. Of course, an appropriate expansion in the vertical direction also needs to be applied.

Paralleling the control synthesis done in previous studies [1,4,5], one can define the perturbation wall-normal velocity to include an inhomogenous part to represent control applied at the upper or lower (or both) wall(s):

$$v' = v_h + \chi \tag{B15}$$

Here, v_h represents the homogeneous solution in which v_h at $y = \pm 1$ is equal to zero, and χ is such that it equals the control input at $y = \pm 1$, $y = -1$, or $y = 1$ (depending on one's choice of control input). This means that the total wall-normal velocity is now described as

$$v(t,x,y,z) = v_c + v_h + \chi$$

The direct state-space form from the discretization described previously is

$$\bar{\boldsymbol{A}}_1\frac{\mathrm{d}\boldsymbol{y}}{\mathrm{d}t} - \bar{\boldsymbol{B}}_2\frac{\mathrm{d}\boldsymbol{u}}{\mathrm{d}t} = \bar{\boldsymbol{A}}_2\boldsymbol{y} + \bar{\boldsymbol{B}}_1\boldsymbol{u} \tag{B16}$$

By a change of variables [1,4,5], Eq. (B16) is transformed into Eq. (12).

References

[1] Joshi, S. S., Speyer, J. L., and Kim, J., "A Systems Theory Approach to the Feedback Stabilization of Infinitesimal and Finite-Amplitude Disturbances in Plane Poiseuille Flow," *Journal of Fluid Mechanics*, Vol. 332, Feb. 1997, pp. 157–184.

[2] Bewley, T. R., and Liu, S., "Optimal and Robust Control and Estimation of Linear Paths to Transition," *Journal of Fluid Mechanics*, Vol. 365, June 1998, pp. 305–349. doi:10.1017/S0022112098001281

[3] Joshi, S. S., Speyer, J. L., and Kim, J., "Finite-Dimensional Optimal Control of Poiseuille Flow," *Journal of Guidance, Control, and Dynamics*, Vol. 22, No. 2, 1999, pp. 340–348. doi:10.2514/2.4383

[4] Cortelezzi, L., and Speyer, J. L., "Robust Reduced-Order Controller of Laminar Boundary Layer Transitions," *Physical Review E*, Vol. 58, No. 2, 1998, pp. 1906–1910. doi:10.1103/PhysRevE.58.1906

[5] Lee, K. H., Cortelezzi, L., Kim, J., and Speyer, J. L., "Application of Robust Reduced-Order Controller to Turbulent Flows for Drag Reduction," *Physics of Fluids*, Vol. 13, No. 5, 2001, pp. 1321–1330. doi:10.1063/1.1359420

[6] Kim, J., "Control of Turbulent Boundary Layers," *Physics of Fluids*, Vol. 15, No. 5, 2003, pp. 1093–1105. doi:10.1063/1.1564095

[7] Högberg, M., Bewley, T. R., and Henningson, D. S., "Linear Feedback Control and Estimation of Transition in Plane Channel Flow," *Journal of Fluid Mechanics*, Vol. 481, April 2003, pp. 149–175. doi:10.1017/S0022112003003823

[8] Hœpffner, J., Brandt, L., and Henningson, D. S., "Transient Growth on Boundary Layer Streaks," *Journal of Fluid Mechanics*, Vol. 537, Aug. 2005, pp. 91–100. doi:10.1017/S0022112005005203

[9] Aamo, O. M., and Krstic, M., *Flow Control by Feedback*, Springer–Verlag, London, 2003, pp. 41–133. doi:10.1007/978-1-4471-3805-1

[10] Min, T., Kang, S. M., Speyer, J. L., and Kim, J., "Sustained Sub-Laminar Drag in a Fully Developed Channel Flow," *Journal of Fluid Mechanics*, Vol. 558, July 2006, pp. 309–319. doi:10.1017/S0022112006000206

[11] Hœpffner, J., and Fukagata, K., "Pumping or Drag Reduction?" *Journal of Fluid Mechanics*, Vol. 635, Sept. 2009, pp. 171–187. doi:10.1017/S0022112009007629

[12] Kim, J., Moin, P., and Moser, R. K., "Turbulence Statistics in Fully Developed Channel Flow at Low Reynolds Number," *Journal of Fluid Mechanics*, Vol. 177, April 1987, pp. 133–166. doi:10.1017/S0022112087000892

[13] Moarref, R., and Jovanovic, M. R., "Controlling the Onset of Turbulence by Streamwise Traveling Waves, Part 1: Receptivity Analysis," *Journal of Fluid Mechanics*, Vol. 663, Nov. 2010, pp. 70–99. doi:10.1017/S0022112010003393

[14] Lieu, B. K., Moarref, R., and Jovanovic, M. R., "Controlling the Onset of Turbulence by Streamwise Traveling Waves, Part 2: Direct Numerical Simulations," *Journal of Fluid Mechanics*, Vol. 663, Nov. 2010, pp. 100–119. doi:10.1017/S002211201000340X

[15] Lee, C., Min, T., and Kim, J., "Stability of a Channel Flow Subject to Wall Blowing and Suction in the Form of a Traveling Wave," *Physics of Fluids*, Vol. 20, No. 10, 2008, Paper 101513. doi:10.1063/1.3006057

[16] Kang, S. M., "Skin-Friction Drag Reduction in Laminar and Turbulent Boundary Layer," Ph.D. thesis, University of California, Los Angeles, Los Angeles, CA, 2006.

[17] Kelly, R. E., "On the Stability of an Inviscid Shear Layer Which is Periodic in Space and Time," *Journal of Fluid Mechanics*, Vol. 27, No. 4, March 1967, pp. 657–689. doi:10.1017/S0022112067002538

[18] Floryan, J. M., "Stability of Wall-Bounded Shear Layers in the Presence of Simulated Distributed Surface Roughness," *Journal of Fluid Mechanics*, Vol. 335, March 1997, pp. 29–55. doi:10.1017/S0022112096004429

[19] Selvarajan, S., Tulapurkara, E. G., and Vasanta Ram, V., "Stability Characteristics of Wavy Walled Channel Flows," *Physics of Fluids*, Vol. 11, No. 3, 1999, pp. 579–589. doi:10.1063/1.869946

[20] Brockett, R. W., *Finite Dimensional Linear Systems*, Wiley, New York, 1970, pp. 46–52.

[21] Bewley, T. R., and Aamo, O. M., "A 'Win-Win' Mechanism for Low-Drag Transients in Controller Two-Dimensional Channel Flow and its Implications for Sustained Drag Reduction," *Journal of Fluid Mechanics*, Vol. 499, Jan. 2004, pp. 183–196. doi:10.1017/S0022112003006852

[22] Lehtomaki, N. A., Sandell, N. R., and Athans, M., "Robustness Results in Linear-Quadratic-Gaussian Based Multivariable Control Designs," *IEEE Transactions on Automatic Control*, Vol. 26, No. 1, Feb. 1981, pp. 75–93. doi:10.1109/TAC.1981.1102565